

Collective dynamics of chemically active particles trapped at a fluid interface

Alvaro Domínguez*

Física Teórica, Universidad de Sevilla, Apdo. 1065, 41080 Sevilla, Spain

P. Malgaretti, M. N. Popescu, and S. Dietrich

Max-Planck-Institut für Intelligente Systeme, Heisenbergstr. 3, 70569 Stuttgart, Germany and

IV. Institut für Theoretische Physik, Universität Stuttgart,

Pfaffenwaldring 57, D-70569 Stuttgart, Germany

(Dated: June 28, 2016)

Chemically active colloids generate changes in the chemical composition of their surrounding solution and thereby induce flows in the ambient fluid which affect their dynamical evolution. Here we study the many-body dynamics of a monolayer of active particles trapped at a fluid-fluid interface. To this end we consider a mean-field model which incorporates the direct pair interaction (including also the capillary interaction which is caused specifically by the interfacial trapping) as well as the effect of hydrodynamic interactions (including the Marangoni flow induced by the response of the interface to the chemical activity). The values of the relevant physical parameters for typical experimental realizations of such systems are estimated and various scenarios, which are predicted by our approach for the dynamics of the monolayer, are discussed. In particular, we show that the chemically-induced Marangoni flow can prevent the clustering instability driven by the capillary attraction.

Introduction.— Chemically active, micron-sized particles are capable of self-induced motility by promoting a chemical reaction in the surrounding solution [1, 2]. Numerous experimental [1–9] and theoretical [10–21] studies have been devoted to the motility mechanisms of such particles. Since the motion is caused by an intricate coupling between the chemical and hydrodynamic flow fields produced by these particles, this kind of colloids may exhibit a very complex behavior — such as the emergence of surface-bounded steady-states [22–26], enhanced motility [27], rheotaxis [28], gravitaxis [29, 30] — when they move near walls or are exposed to external flows or force fields.

The phenomenology becomes even richer if the walls, in addition to their “inert” role as a provider of confinement, are themselves responsive to, e.g., the chemical inhomogeneities induced by the activity of the colloid [31]. A natural realization of this scenario is a fluid–fluid interface, the surface tension of which depends on the distribution of chemicals near the interfacial region. In this case, the spatially nonuniform distribution of chemical components gives rise to Marangoni stresses¹ and the ensuing Marangoni flow in the ambient fluid leads either to self-propulsion along the interface for a particle trapped at the interface [33, 34] or to an effective, long-ranged interaction of the particle with an interface located in its proximity [35].

Naturally the issue arises concerning the collective behavior of chemically active particles forming a monolayer at a responsive fluid–fluid interface. The effective interaction between two particles, a distance d apart, due to

the advection by the induced Marangoni flow is equivalent to a long-ranged interparticle force decaying as $1/d$. The study in Ref. [36] has shown that on large scales this can give rise to a clustering instability similar to the “chemotactic collapse” exhibited by the Keller–Segel model [37] if the chemical activity *increases* the surface tension. However, in general, the particles exhibit also interactions which are not of hydrodynamic nature but determine the equilibrium states. (In the present study, for reasons of simplicity and for this kind of interactions we shall use the notion “equilibrium-like”.) The capillary interaction between particles trapped at a fluid interface is particularly notable [38–40]. In two respects this interaction differs strongly from, e.g., electrostatic double layer or van der Waals interactions: (i) it is a direct consequence of surface tension; (ii) it decays as $1/d$ over a wide range of significant interparticle separations of the colloids and induces a clustering instability formally analogous to a “gravitational collapse” [41, 42] (and equivalent to the chemotactic collapse [43]). These two features are shared with the Marangoni-induced dynamics, and a competition between both effects (i.e., capillarity and Marangoni advection) is conceivable. Furthermore, the particle motion driven by the “equilibrium-like” interactions also induces a flow — formally indistinguishable from a Marangoni-stress driven one — in the ambient fluid, which leads to “anomalous collective diffusion” [44].

Accordingly, in the present study we aim at understanding the collective behavior exhibited by a monolayer of chemically active colloidal particles trapped at an interface in the presence of *both* “equilibrium-like” and hydrodynamic interactions. For this purpose, we employ a theoretical framework developed previously in Refs. [41, 45] for studying the collective dynamics of inert colloids trapped at a fluid interface, and consistently incorporate the simple model of chemical activity as dis-

* dominguez@us.es

¹ We remark that a similar motility mechanism can originate from thermally induced Marangoni flows if the particle is heated (see, e.g., Ref. [32]).

cussed in Refs. [35, 36]. We study the stability of a homogeneous monolayer, with a special focus on the case that the “equilibrium-like” part of the interaction is dominated by the monopolar capillary attraction. Since the capillary attraction is exponentially screened beyond the capillary length λ (which is of the order of millimeter), the chemically induced Marangoni flow eventually dominates at the largest scales. However, on submillimeter scales, the capillary forces (and, more specifically, the advection by the ambient flow driven by them and leading to “anomalous diffusion” [44]) can dominate over the Marangoni flow. For typical experimental conditions, we show that the Marangoni flow can prevent the clustering driven by capillary attraction if the produced chemical species tends to *decrease* the surface tension of the interface.

Theoretical model.— We consider a collection of particles trapped at a flat fluid interface and forming a monolayer. The dynamic evolution of the system is driven by Brownian diffusion; external force fields; “equilibrium-like” particle interactions through direct forces (e.g., hard-core repulsion, electrostatic forces, or, specific to the presence of a fluid interface, capillary forces); and interactions mediated by the surrounding ambient fluid (i.e., in the form of hydrodynamic interactions). The source of the latter is not only the force (i.e., the “hydrodynamic monopole”) acting on each particle, but also the Marangoni stresses at the fluid interface induced by the spatial distribution of a tensioactive chemical species “ A ” which is liberated (or absorbed) by the particles.

In order to describe the collective evolution of the monolayer we assume that the evolution of the areal particle density $\varrho(\mathbf{r}, t)$ occurs on time scales larger than any other process. (In order to keep the notation simple, we shall explicitly indicate the time dependence of ϱ and other variables only when necessary.) Accordingly, one introduces the following fields (here, $\mathbf{r} = (x, y)$ denotes a point at the fluid interface, identified with the plane $z = 0$): the velocity field $\mathbf{v}(\mathbf{r})$ of the monolayer; the (thermodynamic) force per particle $\mathbf{f}(\mathbf{r})$ due to mutual interactions, external force fields, and Brownian diffusion; the number density $c(\mathbf{r}, z)$ of the chemical A in bulk; the velocity field $\mathbf{u}(\mathbf{r}, z)$ in the bulk of the ambient fluid above and below the fluid interface; and the inhomogeneous surface tension $\gamma(\mathbf{r})$ of the fluid interface. (We note that all these fields are also (implicitly) time dependent through their dependence on ϱ .)

The density field obeys the continuity equation for the monolayer, expressing particle number conservation:

$$\frac{\partial \varrho}{\partial t} = -\nabla \cdot (\varrho \mathbf{v}), \quad \nabla := \left(\frac{\partial}{\partial x}, \frac{\partial}{\partial y} \right), \quad (1)$$

with the velocity field $\mathbf{v}(\mathbf{r})$ in the overdamped regime of particle motion in the ambient flow given by

$$\mathbf{v}(\mathbf{r}) = \Gamma(\varrho) \mathbf{f}(\mathbf{r}) + \mathbf{u}(\mathbf{r}, z = 0), \quad (2)$$

where $\Gamma(\varrho)$ is the particle mobility in the monolayer. This velocity field expresses the superposition of the drag by the force and the advection by the ambient flow. Under the assumption of local equilibrium in isothermal conditions, the thermodynamic force $\mathbf{f}(\mathbf{r})$ (i.e., the negative gradient of the chemical potential) can be expressed as

$$\mathbf{f}(\mathbf{r}) = -\nabla \frac{\delta \mathcal{F}[\varrho]}{\delta \varrho(\mathbf{r})} \quad (3)$$

in terms of a free energy functional $\mathcal{F}[\varrho]$ for the monolayer. This functional accounts for the effect of Brownian motion, external force fields, and the “equilibrium-like” interactions between the particles. By construction this force has only an in-plane component; any non-vanishing component of the forces in the direction normal to the interface is exactly canceled by the constraining forces (usually the wetting forces) which impose the trapping at the interfacial plane $z = 0$.

The ambient flow $\mathbf{u}(\mathbf{r}, z)$ is given as the solution of the Stokes equation (describing incompressible flows at low Reynolds number) and it accounts both for the forces acting on the particles and for the Marangoni stresses at the fluid interface [35, 36, 45]:

$$\mathbf{u}(\mathbf{r}, z) = \int d^2 \mathbf{r}' [\varrho(\mathbf{r}') \mathbf{f}(\mathbf{r}') + \nabla' \gamma(\mathbf{r}')] \cdot \mathcal{O}(\mathbf{r} - \mathbf{r}' + z \mathbf{e}_z), \quad (4)$$

with the Oseen tensor

$$\mathcal{O}(\mathbf{R} = \mathbf{r} + z \mathbf{e}_z) = \frac{1}{8\pi\eta_+ |\mathbf{R}|} \left[\mathcal{I} + \frac{\mathbf{R}\mathbf{R}}{|\mathbf{R}|^2} \right], \quad (5)$$

where \mathcal{I} is the identity tensor and η_+ is the arithmetic mean of the dynamical viscosities of the upper and the lower fluid phases, respectively². (Equation (5) is obtained from the general solution given in Ref. [46] upon specializing to the case that the sources of the flow are localized within the plane $z = 0$.)

Following the analysis in Ref. [35], the dependence of the surface tension on the density of the tensioactive chemical at the interface is modeled as

$$\gamma(\mathbf{r}) = \gamma_0 - b_0 [c(\mathbf{r}, z = 0) - c_0], \quad b_0 := -\left. \frac{d\gamma}{dc} \right|_{c=c_0}, \quad (6)$$

where c_0 and γ_0 are given reference values for the density of the species A and the surface tension, respectively. Typically the coefficient b_0 is positive so that the interfacial tension is reduced by the presence of the chemical.

The distribution of the chemical is determined as the stationary solution of the diffusion equation for the corresponding field $c(\mathbf{r}, z)$ with the particles acting as sources (or sinks) of the chemical species, assuming that the advection by the ensuing flows is negligible (i.e., the Péclet

² We use the convention that adjacent vectors without the dot or the cross product sign denotes a dyadic (or tensorial) product.

number of the species A is considered to be very small [33–35]):

$$D \left(\nabla^2 + \frac{\partial^2}{\partial z^2} \right) c = -Q\delta(z)\varrho(\mathbf{r}), \quad (7)$$

where Q is the rate of production (if $Q > 0$) or annihilation (if $Q < 0$), respectively, of molecules of species A per colloidal particle, and D is the diffusion coefficient of the species A in the fluids. For reasons of simplicity and in order to allow for an analytical derivation in closed form, rendering physically intuitive results, we take the diffusion coefficient as well as the solubility of the species to have the same value in both fluids. (Under these conditions, both the field c and its derivatives are continuous at the interfacial plane [35]. This simplifies the problem significantly because the presence of the interface does not influence the distribution of the chemical species.)

Finally, this mathematical model has to be complemented with appropriate boundary conditions. One usually considers (also for reasons of simplicity) an unbounded domain with appropriate boundary conditions at infinity, such as vanishing ambient flow and a fixed current or a fixed chemical potential for the chemical species A .

Equations (1–7) form a closed system which determines the evolution of the particle density field $\varrho(\mathbf{r}, t)$. Before proceeding with the corresponding analysis, three remarks are in order.

(i) The ambient flow $\mathbf{u}(\mathbf{r}, z)$, entering Eq. (2) and being given self-consistently in terms of the particle distribution, represents the effect of the hydrodynamic interactions, i.e., how the ambient flow driven by one particle affects the motion of the other ones. There are two mechanisms leading to a hydrodynamic interaction, which according to Eq. (4) enter on equal footing: one contribution is due to the forces $\mathbf{f}(\mathbf{r})$ acting on the particles, and one is due to the chemical activity of the particles and is represented by the Marangoni stresses $\nabla\gamma(\mathbf{r})$. This flow is computed in the point-particle approximation: only the monopolar (Stokeslet) term, given by the Oseen tensor, is retained, which describes a long-ranged hydrodynamic interaction (the Oseen tensor in Eq. (5) decays $\sim 1/|\mathbf{R}|$). This approximation can be viewed as the dilute limit of the model or, more generally, as a mean-field approximation in which the effect of the short-ranged correlations (in the form of higher-order hydrodynamic multipoles) is incorporated — at this level of description — by means of an effective density-dependence of the rheological parameters of the monolayer as, e.g., the particle mobility Γ [47, 48]. Notwithstanding the common

features just discussed, in the following we shall reserve the notion “hydrodynamic interactions” to those induced by the forces $\mathbf{f}(\mathbf{r})$, as it is common use in the literature, and the effects by the Marangoni stresses will be referred to specifically.

(ii) In Eq. (7) the particles are modeled as monopolar sources of the tensioactive species A . This neglects, for reasons of simplicity, the detailed spatial structure of the production of A on the surface of the particles, e.g. to which extent they are Janus particles. In particular, because of the assumed spherical symmetry (monopolar source), a single particle does not move by self-phoresis nor it is dragged in-plane by the Marangoni flow it induces. Therefore the influence of the particle activity on the dynamics shows up only as a collective effect via the hydrodynamic interactions and the Marangoni flows.

(iii) Equations (1–7) encompass, as limiting cases, two situations addressed recently in the literature. If the particles are not active (i.e., $Q = 0$ in Eq. (7)), one recovers the model introduced in Ref. [44] for the emergence of anomalous diffusion due to the hydrodynamic interactions. If, however, the monolayer is modeled as a two-dimensional (2D) ideal gas and the hydrodynamic interactions are neglected (i.e., if $\mathbf{f} = 0$ in Eq. (4)), the model reduces to the one studied in Ref. [36].

Linear stability of the homogeneous state.— We restrict the discussion to the case in which the external force fields have vanishing in-plane components (e.g., gravity for a horizontal interface). Therefore they do not contribute to $\mathbf{f}(\mathbf{r})$ and the whole spatial dependence of the free energy \mathcal{F} in Eq. (3) enters only via the density field. In this case, the model described by Eqs. (1–7) has a stationary solution given by the homogeneous distribution $\varrho(\mathbf{r}, t) = \varrho_0$. In the following we analyze the linear stability of this state with respect to small perturbations $\delta\varrho(\mathbf{r}, t) := \varrho(\mathbf{r}, t) - \varrho_0$.

By linearizing the governing equations we obtain the following system of equations which determines the evolution of the perturbation $\delta\varrho$:

$$\frac{\partial \delta\varrho}{\partial t} = -\varrho_0 \nabla \cdot [\Gamma_0 \delta\mathbf{f}(\mathbf{r}) + \delta\mathbf{u}(\mathbf{r}, z=0)], \quad (8a)$$

where $\Gamma_0 := \Gamma(\varrho_0)$,

$$\delta\mathbf{f}(\mathbf{r}) = -\nabla \int d^2\mathbf{r}' \frac{\delta^2 \mathcal{F}[\varrho]}{\delta\varrho(\mathbf{r})\delta\varrho(\mathbf{r}')} \Big|_{\varrho=\varrho_0} \delta\varrho(\mathbf{r}'), \quad (8b)$$

and

$$\delta\mathbf{u}(\mathbf{r}, z) = \int d^2\mathbf{r}' [\varrho_0 \delta\mathbf{f}(\mathbf{r}') - b_0 \nabla' \delta c(\mathbf{r}', z=0)] \cdot \mathcal{O}(\mathbf{r} - \mathbf{r}' + z\mathbf{e}_z), \quad (8c)$$

with δc solving

$$D \left(\nabla^2 + \frac{\partial^2}{\partial z^2} \right) \delta c = -Q\delta(z)\delta\varrho(\mathbf{r}). \quad (8d)$$

Assuming that at infinity the perturbations vanish suffi-

ciently fast, one can introduce the 2D Fourier transforms of the fields:

$$\delta \varrho_{\mathbf{k}}(t) := \int d^2 \mathbf{r} e^{-i\mathbf{k} \cdot \mathbf{r}} \delta \varrho(\mathbf{r}, t) \quad (9)$$

and similarly for the others. With these Eq. (8a) turns into

$$\frac{\partial \delta \varrho_{\mathbf{k}}}{\partial t} = -i\mathbf{k} \cdot [\Gamma_0 \varrho_0 \delta \mathbf{f}_{\mathbf{k}} + \varrho_0 \delta \mathbf{u}_{\mathbf{k}}(z=0)]. \quad (10)$$

The absence of in-plane contributions from external fields implies translational invariance and isotropy for the dynamics at the interface, which allows us to introduce a function $\hat{\mathcal{D}}_0(r)$ as

$$\left. \frac{\delta^2 \mathcal{F}[\varrho]}{\delta \varrho(\mathbf{r}) \delta \varrho(\mathbf{r}')} \right|_{\varrho=\varrho_0} := \frac{1}{\Gamma_0 \varrho_0} \hat{\mathcal{D}}_0(|\mathbf{r} - \mathbf{r}'|). \quad (11)$$

Therefore the convolution on the right hand side of Eq. (8b) is given by

$$\delta \mathbf{f}_{\mathbf{k}} = -i\mathbf{k} \frac{\mathcal{D}_0(k)}{\Gamma_0 \varrho_0} \delta \varrho_{\mathbf{k}}, \quad (12)$$

where

$$\mathcal{D}_0(k) := \int d^2 \mathbf{r} e^{-i\mathbf{k} \cdot \mathbf{r}} \hat{\mathcal{D}}_0(r) \quad (13)$$

is the wavenumber-dependent coefficient of 2D collective diffusion of the monolayer in the absence of (long-ranged) hydrodynamic interactions (i.e., for $\delta \mathbf{u} \equiv 0$ in Eq. (8a)). The value $\mathcal{D}_0(k \rightarrow 0)$ is related to the isothermal compressibility of the monolayer in the equilibrium state [49]; for instance, for an ideal gas at temperature T one has $\mathcal{F}_{\text{ideal}}[\varrho] = k_B T \int d^2 \mathbf{r} \varrho(\mathbf{r}) [\ln[\Lambda^2 \varrho(\mathbf{r})] - 1]$ (where Λ and k_B are de Broglie's thermal length and Boltzmann's constant, respectively) so that $\mathcal{D}_0(k) = \Gamma_0 k_B T$.

By using the known three-dimensional (3D) Fourier transform [50] of the Oseen tensor one obtains its 2D Fourier transform as

$$\begin{aligned} \int d^2 \mathbf{r} e^{-i\mathbf{k} \cdot \mathbf{r}} \mathcal{O}(\mathbf{r} + z\mathbf{e}_z) = \\ \int_{-\infty}^{+\infty} \frac{dq}{2\pi} e^{iqz} \frac{1}{\eta_+(k^2 + q^2)} \left[\mathcal{I} - \frac{(\mathbf{k} + q\mathbf{e}_z)(\mathbf{k} + q\mathbf{e}_z)}{k^2 + q^2} \right] = \\ \frac{e^{-k|z|}}{4\eta_+ k} \left[2\mathcal{I} - (1 - k|z|)\mathbf{e}_z \mathbf{e}_z - (1 + k|z|)\frac{\mathbf{k}\mathbf{k}}{k^2} \right], \end{aligned} \quad (14)$$

so that the convolution on the rhs of Eq. (8c) leads to

$$i\mathbf{k} \cdot \delta \mathbf{u}_{\mathbf{k}}(z=0) = \frac{i\mathbf{k}}{4\eta_+ k} \cdot [\varrho_0 \delta \mathbf{f}_{\mathbf{k}} - i\mathbf{k} b_0 \delta c_{\mathbf{k}}(z=0)]. \quad (15)$$

Equation (8d) can be solved via the 3D Fourier transform of δc from which one determines the 2D Fourier transform $\delta c_{\mathbf{k}}(z=0)$ (analogously to the above calculation for the

Oseen tensor)³

$$\delta c_{\mathbf{k}}(z=0) = \int_{-\infty}^{+\infty} \frac{dq}{2\pi} \frac{Q \delta \varrho_{\mathbf{k}}}{D(k^2 + q^2)} = \frac{Q}{2Dk} \delta \varrho_{\mathbf{k}}. \quad (16)$$

By inserting Eqs. (12–16) into Eq. (10), one finally arrives at

$$\frac{\partial \delta \varrho_{\mathbf{k}}}{\partial t} = \frac{\delta \varrho_{\mathbf{k}}}{\tau_k}, \quad \frac{1}{\tau_k} = -k^2 \mathcal{D}_0(k) g(k) - \frac{\text{sign}(Q b_0)}{T_{\text{surf}}}, \quad (17)$$

where

$$g(k) := 1 + \frac{1}{L_{\text{hydro}} k}, \quad (18)$$

with the length scale [44]

$$L_{\text{hydro}} := \frac{4\eta_+ \Gamma_0}{\varrho_0} \quad (19)$$

and the time scale [36]

$$T_{\text{surf}} := \frac{8\eta_+ D}{|Q b_0| \varrho_0}. \quad (20)$$

Equation (17) allows one to transparently identify the various driving mechanisms. The Marangoni stresses induce growth (if $Q b_0 < 0$) or decay (if $Q b_0 > 0$) of the perturbation at the same rate $1/T_{\text{surf}}$ at all length scales, i.e., independent of k . Since typically $b_0 > 0$, the associated Marangoni flow leads to an effective repulsive interaction between the particles if they are sources ($Q > 0$) of the tensioactive agent. The diffusive dynamics is encoded in $\mathcal{D}_0(k)$, while the factor $g(k)$ accounts for the (long-ranged part of the) hydrodynamic interactions. Since $g(k) > 0$, the generic effect of these interactions is to reduce the time scales associated with the diffusive evolution. This is at variance with the usual effect of the short-ranged parts of the hydrodynamic interactions, which tend to reduce the mobility Γ_0 (at least for hard-spheres; the presence of direct short-ranged attractive interactions can favor an increase of the mobility [51, 52]). Furthermore, as discussed in Ref. [44], the factor $g(k)$ is responsible for the anomalous diffusion on length scales above L_{hydro} : $g(k \rightarrow 0)$ diverges, which implies a rate $\sim k \mathcal{D}_0(0)$ for the evolution of the largest scales and thus amounts to a superdiffusive behavior. This divergence can be traced back to the dimensionality mismatch between the 2D dynamics of the confined colloid and the 3D hydrodynamic interactions mediated by the unconfined adjacent fluids.

³ The divergences both in Eq. (14) and in Eq. (16) as $k \rightarrow 0$ reflect the slow spatial decay of the Green functions of the Stokes equation and the Poisson equation (7), respectively. They pose no mathematical difficulty because the Green functions are convoluted with the perturbation fields, which are taken to vanish at infinity sufficiently fast.

Discussion.— First, we consider the case that the direct particle interactions are short-ranged, so that on large length scales k^{-1} well above the relevant microscopic ones (e.g., the correlation length or the mean interparticle separation), one can approximate $\mathcal{D}_0(k) \approx \mathcal{D}_0(0) =: \mathcal{D}_{\text{short}}$ (with the subscript “short” referring to the case of short-ranged interactions). Accordingly, Eq. (17) states that for modes with sufficiently small values of k the dynamics is always dominated by the effect of the Marangoni flow. Therefore, even if the homogeneous state is thermodynamically stable ($\mathcal{D}_{\text{short}} > 0$), for $Qb_0 < 0$ a clustering instability is predicted. This instability is driven by the Marangoni flow and occurs for modes with sufficiently small wavenumbers,

$$k < k_c := \frac{1}{2L_{\text{hydro}}} \left[\sqrt{1 + \left(\frac{2L_{\text{hydro}}}{L_{\text{surf}}} \right)^2} - 1 \right], \quad (21)$$

where k_c is the positive solution of $1/\tau_k = 0$ in Eq. (17), and the length scale L_{surf} is given by

$$L_{\text{surf}} := \sqrt{\mathcal{D}_{\text{short}} T_{\text{surf}}}. \quad (22)$$

If $L_{\text{hydro}} \gg L_{\text{surf}}$, this expression reduces to $k_c \approx 1/L_{\text{surf}}$ and the regime (discussed recently in Ref. [36]) in which the hydrodynamic interactions are neglected (i.e., $g(k) \approx 1$ in Eq. (17)) is recovered. In the opposite limit, $L_{\text{hydro}} \ll L_{\text{surf}}$, this critical wavenumber is reduced by a large factor down to $k_c \approx L_{\text{hydro}}/L_{\text{surf}}^2$ because the diffusion (enhanced into super-diffusion by the hydrodynamic interactions) is more effective in stabilizing the homogeneous state.

We now consider the case that the particles interact among each other through capillary forces due to deformations of the fluid interface. This choice of the interaction is particularly interesting because, like the Marangoni stresses, these forces are specific to the presence of a fluid interface and have a strength related to the value of the surface tension. The capillary interaction can be modeled analogously to direct electrostatic interactions in the limit that the deviation of the interface from the flat state is small [53]. An experimentally relevant example is the one in which the interfacial deformation arises because each particle experiences a vertical force $F\mathbf{e}_z$ due to an external agent such as buoyancy or an external electric field normal to the interface [54]. (As remarked below Eq. (3), only in-plane interactions contribute to the force \mathbf{f} ; thus \mathbf{F} , which is normal to the interface, does not affect \mathbf{f} .) In this case, and within the point-particle approximation, the particles can be described as so-called “capillary monopoles”. The associated interaction is attractive and has a range of the order of the capillary length⁴ λ_0 . For typical fluid interfaces

this length is of the order of millimeter. Therefore, for colloidal-sized particles this capillary monopolar interaction can be successfully addressed within a mean-field approximation, leading to [41]

$$\mathcal{D}_0(k) = -\frac{1}{T_{\text{Jeans}}} \frac{\lambda_0^2}{1 + (\lambda_0 k)^2}, \quad (23)$$

with the characteristic time (Jeans time)

$$T_{\text{Jeans}} := \frac{\gamma_0}{\Gamma_0 F^2 \varrho_0}. \quad (24)$$

(This result follows by assuming a spatially constant surface tension γ_0 . Within the linear approximation of small perturbations $\delta\rho$ considered here, the correction to the capillary interaction due to a spatially varying surface tension does not contribute.) The fact that the range λ_0 is much larger than the interparticle separation sets this interaction apart from the other ones mentioned above: there is a whole range of wavenumbers k with $k \rightarrow 0$ but $\lambda_0 k \gg 1$ for which the continuum description we have introduced is valid and yet the approximation $\mathcal{D}_0(k) \sim k^{-2}$ (Eq. (23)) holds. In this intermediate range of scales this formal divergence is a signature of the long-ranged nature of the monopolar capillary attraction (which is formally analogous to 2D Newtonian gravity [42]). In Eq. (17) it leads to a k -independent contribution like the one by the Marangoni flow, thus emphasizing the importance of studying the possible competition between these two effects. We remark that Eq. (23) describes an instability ($\mathcal{D}_0(k) < 0$, the so-called “capillary collapse”) because for reasons of simplicity we have neglected the stabilizing effect of Brownian diffusion and of possible short-ranged repulsions. (In Eq. (23) this would appear as an additive term $\mathcal{D}_{\text{short}}$ and it would become effective on length scales below the Jeans length $L_{\text{Jeans}} := \sqrt{\mathcal{D}_{\text{short}} T_{\text{Jeans}}}$ [41]).

As discussed above, the sign of the product Qb_0 determines whether the effective interactions due to the Marangoni flows are attractive or repulsive. First, we consider the case $Qb_0 > 0$, so that the repulsive effect of the Marangoni flow could actually counterbalance the capillary instability. In this case, the combination of Eqs. (17) and (23) gives the growth rate

$$\frac{1}{\tau_k} = \frac{1}{T_{\text{Jeans}}} \frac{(\lambda_0 k)^2}{1 + (\lambda_0 k)^2} \left[1 + \frac{1}{L_{\text{hydro}} k} \right] - \frac{1}{T_{\text{surf}}}. \quad (25)$$

Thus, the relevant physical dimensionless parameters are the ratio $L_{\text{hydro}}/\lambda_0$, which controls the importance of the anomalous-diffusion effect on the capillary-driven dynamics, and the ratio $T_{\text{Jeans}}/T_{\text{surf}}$, which measures the relative strength of the capillary forces and the Marangoni flows. The growth rate τ_k^{-1} is illustrated in Fig. 1(a), which allows one to straightforwardly infer the possible scenarios.

On scales $k \ll \lambda_0^{-1}$, the capillary interaction is screened and the behavior thus corresponds to the case discussed

⁴ The capillary length is given by $\lambda_0 = \sqrt{\gamma_0/(g\Delta\rho)}$, where γ_0 is the surface tension, g is the acceleration of gravity, and $\Delta\rho$ is the mass density contrast between the coexisting fluids.

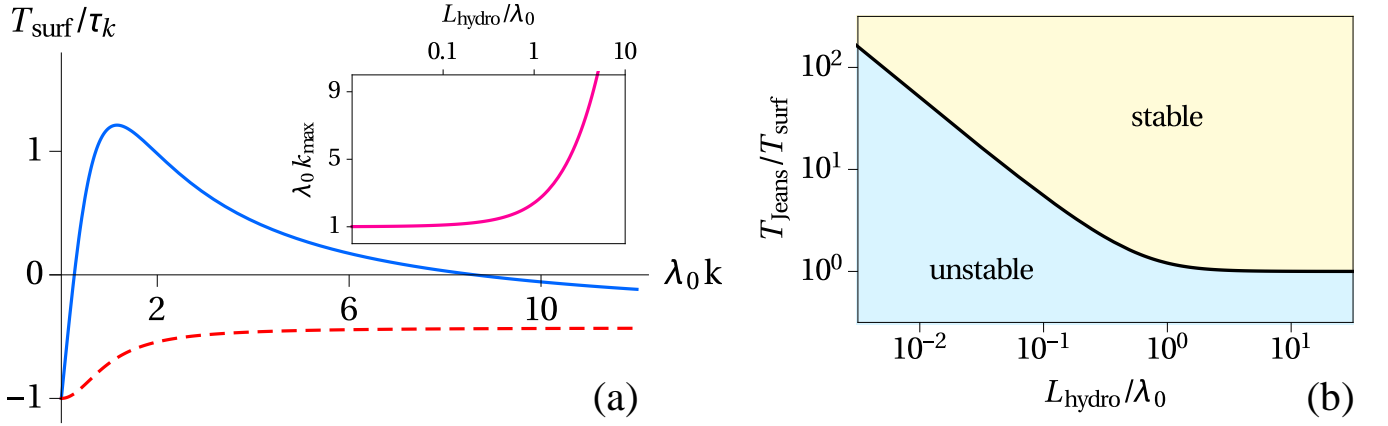


FIG. 1. (a) The growth rate τ_k^{-1} (solid blue line, Eq. (25)) for $Qb_0 > 0$ and the particular parameter choices $L_{\text{hydro}}/\lambda_0 = 0.15$ and $T_{\text{Jeans}}/T_{\text{surf}} = 1.75$. One observes a range of modes with $\lambda_0 k \sim 1$ which are unstable ($\tau_k^{-1} > 0$). For comparison, the dashed red line shows τ_k^{-1} for $L_{\text{hydro}} \rightarrow \infty$; in this case all modes are stable. The inset shows the value k_{max} of the wavenumber at which the growth rate is maximum (see Eq. (26)). (b) Stability diagram in the parameter space spanned by the ratios $L_{\text{hydro}}/\lambda_0$ and $T_{\text{Jeans}}/T_{\text{surf}}$. The separatrix is determined by $\tau_{k_{\text{max}}}^{-1} = 0$. Accordingly, “stable” (“unstable”) means that all modes (some modes) are stable (unstable) within the present linear stability analysis.

above with $\mathcal{D}_0(k) \approx \mathcal{D}_0(0) = -\lambda_0^2/T_{\text{Jeans}}$ finite, i.e., the stabilizing effect of the Marangoni flow dominates. However, on scales $k \gtrsim \lambda_0^{-1}$ the system can be destabilized by the capillary forces; this occurs if the maximum of the curve in Fig. 1(a) lies above zero. The wavenumber k_{max} of the position of the maximum is given as

$$\lambda_0 k_{\text{max}} = \frac{L_{\text{hydro}}}{\lambda_0} + \sqrt{1 + \left(\frac{L_{\text{hydro}}}{\lambda_0}\right)^2}, \quad (26)$$

(see the inset in Fig. 1(a)). The boundary of stability in the parameter space is given by the condition $\tau_{k_{\text{max}}}^{-1} = 0$, see Fig. 1(b). When $L_{\text{hydro}} \ll \lambda_0$, which is the most natural case for a colloidal monolayer (see, c.f., Eq. (32)), the effect of the long-ranged hydrodynamic interactions on the capillary-driven dynamics is important. In this limit one has $\lambda_0 k_{\text{max}} \approx 1$, and the computation of $\tau_{k_{\text{max}}}$ shows that the homogeneous state is stabilized by the Marangoni flow against capillary collapse if

$$\frac{T_{\text{Jeans}}}{T_{\text{surf}}} > \frac{\lambda_0}{2L_{\text{hydro}}} (\gg 1). \quad (27)$$

This inequality follows from requiring that $\tau_{k_{\text{max}}}$ is negative. On the other hand, if this inequality does not hold, an intermediate range of length scales are unstable, with the modes $k \approx \lambda_0^{-1}$ growing the fastest. Although this is reminiscent of the early stages of spinodal decomposition during phase separation, further work is required in order to assess to what extent the nonlinear dynamical evolution is comparable with a coarsening scenario.

The specific signature brought about by the hydrodynamic interactions can be identified by comparing their influence with the predictions in the opposite limit $L_{\text{hydro}} \gg \lambda_0$, so that for the wavenumbers $k \gtrsim \lambda_0^{-1}$, for which the capillary instability is relevant, one can

neglect the effect of the hydrodynamic interactions (by setting $g(k) \rightarrow 1$ in Eq. (17)). The stability diagram in Fig. 1 shows that in this latter case the conditions, under which stabilization of the homogeneous distribution by the Marangoni flow occurs, are less stringent: $T_{\text{Jeans}}/T_{\text{surf}} > 1$ is sufficient. If a mode is unstable, there is usually a broad range of wavenumbers, $1 \lesssim \lambda_0 k \lesssim \lambda_0 k_{\text{max}} \approx 2L_{\text{hydro}}/\lambda_0$, for which the corresponding modes all grow roughly at the same rate (as in the case of the purely capillary instability [41]).

We finally succinctly remark on the case $Qb_0 < 0$: both capillarity and Marangoni flows induce an interparticle attraction and thus destabilize the homogeneous state. The two regimes, in which either one or the other mechanism is dominant, can be visualized from a diagram which has an appearance similar to Fig. 1(b), with the alternative reading that it depicts the parameter regions where clustering is driven predominantly either by capillary attraction (in the region labeled “unstable”, as before) or by the Marangoni flows (in the region labeled “stable”).

Numerical estimates.— In order to complement the theoretical analysis, here we discuss the expected values of the parameters $T_{\text{Jeans}}/T_{\text{surf}}$ and $L_{\text{hydro}}/\lambda_0$ for typical experimental configurations at room temperature. A particle is characterized by its radius R , the chemical activity Q , and the capillary monopole F . We introduce the dimensionless parameter q , which compares the strength of the Marangoni flow with the Brownian motion [35], and the dimensionless parameter W_{cap} , which compares the strength of the inter-particle potential due to capillary attraction with the thermal energy:

$$q_R := \frac{3Qb_0 R}{32Dk_B T}, \quad W_{\text{cap}} := \frac{F^2}{2\pi\gamma_0 k_B T}. \quad (28)$$

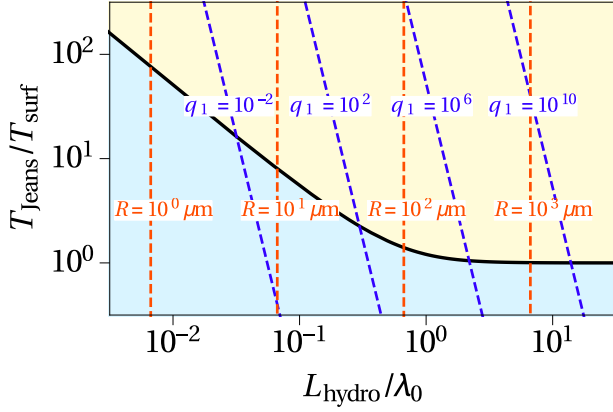


FIG. 2. Plot of the iso- R and iso- q_1 lines in the stability diagram for a monolayer with packing fraction $\phi = 0.1$ at an interface with capillary length $\lambda_0 = 1$ mm.

We also invoke the Stokes mobility for a single particle:

$$\Gamma_0 = \frac{1}{6\pi\eta_+ R}. \quad (29)$$

(Although we are dealing with monolayers, it is known that for colloids in bulk solution Eq. (29) provides a reasonable, order-of-magnitude estimate of the mobility, which depends on the density and the interactions [51, 52].) From Eqs. (20) and (24) one obtains the ratio

$$\frac{T_{\text{Jeans}}}{T_{\text{surf}}} = \frac{4|q_R|}{W_{\text{cap}}}. \quad (30)$$

For colloidal particles at an air–water or an oil–water interface ($\gamma_0 \sim 0.05$ N/m), buoyancy effects lead to an estimate for the capillary force in the order of $W_{\text{cap}} \sim 10^{-6} \times (R/\mu\text{m})^6$ [41], so that

$$\frac{T_{\text{Jeans}}}{T_{\text{surf}}} \sim 4 \times 10^6 \times |q_1| \left(\frac{R}{\mu\text{m}} \right)^{-5}, \quad (31)$$

where $q_1 := q_R(R = 1 \mu\text{m})$ (see Eq. (28)). The sensitive dependence of the capillary monopole on the particle size is transferred to this ratio. The hydrodynamic length scale L_{hydro} can be estimated from Eqs. (19) and (29) as

$$\frac{L_{\text{hydro}}}{\lambda_0} = \frac{2}{3\phi} \frac{R}{\lambda_0}, \quad (32)$$

where $\phi = \pi R^2 \varrho_0$ is the 2D packing fraction of the monolayer. For a not too dilute monolayer of colloidal particles, Eq. (32) predicts that $L_{\text{hydro}}/\lambda_0$ is very small.

Figure 2 shows the curves of constant R , as well as those of constant q_1 , superimposed on the stability diagram for a not too dilute monolayer ($\phi = 0.1$) and with

the order-of-magnitude choice $\lambda_0 = 1$ mm. One observes that an increase in the chemical activity (i.e., the value of q_1) at constant R or a reduction in R at constant chemical activity promote stability of the homogeneous state. As an illustration, the active particles described in Ref. [55] have $Q/(4\pi R^2) \sim 10^{-3}$ mol/(s \times m²) (corresponding to platinum-covered particles catalyzing the decomposition of peroxide into water and oxygen, which is weakly tensioactive). This leads to a small value $|q_1| \sim 10^{-2}$ at an air–water interface. However, switching to a liquid–liquid interface (for which the diffusivity D of oxygen is strongly reduced), enhances the influence of the chemical activity up to $|q_1| \sim 10^2$ [35] and the Marangoni flows can stabilize the homogeneous monolayer even for rather large particles.

As a final remark, we notice that Brownian diffusion sets a lower limit on the particle size for the relevance of the capillary attraction: since $\mathcal{D}_{\text{short}} = \Gamma_0 k_B T$, the Jeans length is $L_{\text{Jeans}} = \sqrt{\Gamma_0 k_B T T_{\text{Jeans}}} = R/\sqrt{2\phi W_{\text{cap}}}$, which becomes larger than the capillary length $\lambda_0 = 1$ mm for radii below $1 \mu\text{m}$.

Conclusions.— We have presented a continuum description which extends previous studies [36, 41, 44] to the case of the dynamics of a monolayer of chemically active colloidal particles trapped at a fluid interface. The model accounts for capillary and hydrodynamic interactions, the latter including the flow induced *both* by the particle motion and by the response of the interface to the chemical activity (i.e., Marangoni flows). The model is a mean-field theory, which is valid for the monopolar contribution to the capillary and hydrodynamic interactions. Our analysis of the linear stability of the homogeneous state revealed a novel stabilization mechanism against clustering driven by capillary attraction, which is due to the induced Marangoni flows (giving rise to repulsive effective interactions). Therefore this mechanism is a feature specific to the “chemically active” nature of the particles and is operational at all length-scales, provided the ratio $T_{\text{Jeans}}/T_{\text{surf}}$ (Eqs. (24) and (20)) of characteristic times is sufficiently large (see Fig. 1(b)). Our numerical estimates indicate that for typical experimental setups this can be the case (see Fig. 2). If this ratio is too small, the perturbations at the long and the very short wavelengths are stabilized by the Marangoni flows, but an intermediate range of length scales are unstable with the modes $k \approx \lambda_0^{-1}$ growing the fastest (see Fig. 1(a)). These findings lend themselves to be explored further by employing numerical studies of the full dynamics.

Acknowledgements.— A.D. acknowledges support by the Spanish Government through Grant FIS2014-53808-P (partially financed by FEDER funds). Support from the COST Action MP 1305 Flowing matter is gratefully acknowledged by the authors.

- Chem. Chem. Phys. **12**, 1423 (2010).
- [3] S. Ebbens, M.-H. Tu, J. R. Howse, and R. Golestanian, Phys. Rev. E **85**, 020401 (2012).
 - [4] T.-C. Lee, M. Alarcón-Correa, C. Miksch, K. Hahn, J. G. Gibbs, and P. Fischer, Nano Letters **14**, 2407 (2014).
 - [5] S. Sánchez, L. Soler, and J. Katuri, Angew. Chem. Int. Ed. **54**, 1414 (2015).
 - [6] L. Baraban, M. Tasinkevych, M. N. Popescu, S. Sánchez, S. Dietrich, and O. G. Schmidt, Soft Matter **8**, 48 (2012).
 - [7] S. Ebbens, D. A. Gregory, G. Dunderdale, J. R. Howse, Y. Ibrahim, T. B. Liverpool, and R. Golestanian, EPL **106**, 58003 (2014).
 - [8] A. Brown and W. Poon, Soft Matter **10**, 4016 (2014).
 - [9] X. Wang, M. In, C. Blanc, M. Nobili, and A. Stocco, Soft Matter **11**, 7376 (2015).
 - [10] R. Golestanian, T. B. Liverpool, and A. Ajdari, Phys. Rev. Lett. **94**, 220801 (2005).
 - [11] R. Golestanian, T. B. Liverpool, and A. Ajdari, New J. Phys. **9**, 126 (2007).
 - [12] G. R. Rückner and R. Kapral, Phys. Rev. Lett. **98**, 150603 (2007).
 - [13] F. Jülicher and J. Prost, Eur. Phys. J. E **29**, 27 (2009).
 - [14] M. N. Popescu, M. Tasinkevych, and S. Dietrich, EPL **95**, 28004 (2011).
 - [15] R. Kapral, J. Chem. Phys. **138**, 202901 (2013).
 - [16] B. ten Hagen, S. van Teeffelen, and H. Löwen, J. Phys.: Condens. Matter **23**, 194119 (2011).
 - [17] S. Michelin and E. Lauga, Eur. Phys. J. E **38**, 7 (2015).
 - [18] B. ten Hagen, F. Kümmel, R. Wittkowski, D. Takagi, H. Löwen, and C. Bechinger, Nature Comm. **5**, 4829 (2014).
 - [19] J. Elgeti, R. G. Winkler, and G. Gompper, Rep. Prog. Phys. **78**, 056601 (2015).
 - [20] A. Zöttl and H. Stark, J. Phys.: Condens. Matter **28**, 253001 (2016).
 - [21] J. de Graaf, G. Rempfer, and C. Holm, IEEE Trans. NanoBiosci. **14**, 272 (2015).
 - [22] J. Palacci, S. Sacanna, A. S. Steinberg, D. J. Pine, and P. M. Chaikin, Science **339**, 936940 (2013).
 - [23] W. E. Usual, M. N. Popescu, S. Dietrich, and M. Tasinkevych, Soft Matter **11**, 434 (2015).
 - [24] S. Das, A. Garg, A. I. Campbell, J. Howse, A. Sen, D. Velegol, R. Golestanian, and S. J. Ebbens, Nature Comm. **6**, 8999 (2015).
 - [25] J. Simmchen, J. Katuri, W. E. Usual, M. N. Popescu, M. Tasinkevych, and S. Sánchez, Nature Comm. **7**, 10598 (2016).
 - [26] A. Mozaffari, N. Sharifi-Mood, J. Koplik, and C. Maldarelli, Phys. Fluids **28**, 053107 (2016).
 - [27] P. Magaretti, M. N. Popescu, and S. Dietrich, Soft Matter **12**, 4007 (2016).
 - [28] W. E. Usual, M. N. Popescu, S. Dietrich, and M. Tasinkevych, Soft Matter **11**, 6613 (2015).
 - [29] A. I. Campbell and S. J. Ebbens, Langmuir **29**, 14066 (2013).
 - [30] M. Enculescu and H. Stark, Phys. Rev. Lett. **107**, 058301 (2011).
 - [31] W. Usual, M. Popescu, S. Dietrich, and M. Tasinkevych, Phys. Rev. Lett. , (in press) (2016).
 - [32] A. Würger, J. Fluid Mech. **752**, 589 (2014).
 - [33] A. Lauga and A. Davis, J. Fluid Mech. **705**, 120 (2011).
 - [34] H. Masoud and H. A. Stone, J. Fluid Mech. **741**, R4 (2014).
 - [35] A. Domínguez, P. Magaretti, M. N. Popescu, and S. Dietrich, Phys. Rev. Lett. **116**, 078301 (2016).
 - [36] H. Masoud and M. J. Shelley, Phys. Rev. Lett. **112**, 128304 (2014).
 - [37] E. Keller and L. Segel, J. Theor. Biol. **26**, 399 (1970).
 - [38] P. A. Kralchevsky and K. Nagayama, Adv. Coll. Interface Sci. **85**, 145 (2000).
 - [39] M. Oettel and S. Dietrich, Langmuir **24**, 1425 (2008).
 - [40] A. Domínguez, “Structure and functional properties of colloidal systems,” (CRC Press, Boca Raton, 2010) pp. 31–59.
 - [41] A. Domínguez, M. Oettel, and S. Dietrich, Phys. Rev. E **82**, 011402 (2010).
 - [42] J. Bleibel, A. Domínguez, M. Oettel, and S. Dietrich, Soft Matter **10**, 4091 (2014).
 - [43] P.-H. Chavanis and C. Sire, Physica A **387**, 4033 (2008).
 - [44] J. Bleibel, A. Domínguez, F. Günther, J. Harting, and M. Oettel, Soft Matter **10**, 2945 (2014).
 - [45] J. Bleibel, A. Domínguez, and M. Oettel, J. Phys.: Condens. Matter **27**, 194113 (2015).
 - [46] R. B. Jones, B. U. Felderhof, and J. M. Deutch, Macromolecules **8**, 680 (1975).
 - [47] P. Nozières, Physica A **147**, 219 (1987).
 - [48] B. U. Felderhof, Physica A **153**, 217 (1988).
 - [49] J. K. G. Dhont, *An Introduction to Dynamics of Colloids* (Elsevier Science, Amsterdam, 1996).
 - [50] S. Kim and S. J. Karrila, *Microhydrodynamics: Principles and Selected Applications* (Butterworth-Heinemann, Boston, 1991).
 - [51] A. Moncho-Jordá, A. A. Louis, and J. T. Padding, Phys. Rev. Lett. **104**, 068301 (2010).
 - [52] E. Lattuada, S. Buzzaccaro, and R. Piazza, Phys. Rev. Lett. **116**, 038301 (2016).
 - [53] A. Domínguez, M. Oettel, and S. Dietrich, J. Chem. Phys. **128**, 114904 (2008).
 - [54] N. Aubry, P. Singh, M. Janjua, and S. Nudurupati, Proc. Nat. Acad. Sci. USA **105**, 3711 (2008).
 - [55] W. F. Paxton, K. C. Kistler, C. C. Olmeda, A. Sen, S. K. S. Angelo, Y. Cao, T. E. Mallouk, P. E. Lammert, and V. H. Crespi, J. Am. Chem. Soc. **126**, 13424 (2004).